Published in final edited form as:
Cancer Res. 2006 November 1; 66(21): 10586–10593.

Eradication of Tumor Colonization and Invasion by a B Cell–Specific Immunotoxin in a Murine Model for Human Primary Intraocular Lymphoma

Zhuqing Li[1], **Sankaranarayana P. Mahesh**[1], **De Fen Shen**[1], **Baoying Liu**[1], **Willie O. Siu**[1], **Frank S. Hwang**[1], **Qing-Chen Wang**[2], **Chi-Chao Chan**[1], **Ira Pastan**[2], and **Robert B. Nussenblatt**[1]

[1]*Laboratory of Immunology, National Eye Institute, NIH, Bethesda, Maryland* [2]*Laboratory of Molecular Biology, National Cancer Institute, NIH, Bethesda, Maryland*

Abstract

Human primary intraocular lymphoma (PIOL) is predominantly a B cell–originated malignant disease with no appropriate animal models and effective therapies available. This study aimed to establish a mouse model to closely mimic human B-cell PIOL and to test the therapeutic potential of a recently developed immunotoxin targeting human B-cell lymphomas. Human B-cell lymphoma cells were intravitreally injected into severe combined immunodeficient mice. The resemblance of this tumor model to human PIOL was examined by fundoscopy, histopathology, immunohistochemistry, and evaluated for molecular markers. The therapeutic effectiveness of immunotoxin HA22 was tested by injecting the drug intravitreally. Results showed that the murine model resembles human PIOL closely. Pathologic examination revealed that the tumor cells initially colonized on the retinal surface, followed by infiltrating through the retinal layers, expanding preferentially in the subretinal space, and eventually penetrating through the retinal pigment epithelium into the choroid. Several putative molecular markers for human PIOL were expressed *in vivo* in this model. Tumor metastasis into the central nervous system was also observed. A single intravitreal injection of immunotoxin HA22 after the establishment of the PIOL resulted in complete regression of the tumor. This is the first report of a murine model that closely mimics human B-cell PIOL. This model may be a valuable tool in understanding the molecular pathogenesis of human PIOL and for the evaluation of new therapeutic approaches. The results of B cell–specific immunotoxin therapy may have clinical implications in treating human PIOL.

Introduction

Primary intraocular lymphoma (PIOL) is considered a subset of primary CNS (central nervous system) lymphoma (PCNSL) and often masquerades as uveitis. Although relatively less common than other forms of lymphoma, there has been a steady increase of PCNSL over the last two decades (1) despite some recent data suggesting that the annual incidence may be stabilizing (2). It has been estimated that the incidence of PCNSL has risen from 0.04 of 100,000 to 0.3 of 100,000 (1,3) in the immunocompetent population, and accounts for 2.7% of primary brain tumors (4). In persons with AIDS, there is a greatly increased risk (3,600-fold higher) of developing PCNSL compared with the general population (3).

Requests for reprints: Robert B. Nussenblatt, Laboratory of Immunology, National Eye Institute, NIH, Building 10, Room 10N112, 9000 Rockville Pike, Bethesda, MD 20892. Phone: 301-496-3123; Fax: 301-480-1122; E-mail: DrBob@nei.nih.gov.

Note: Supplementary data for this article are available at Cancer Research Online (http://cancerres.aacrjournals.org/).

Although it can be T cell in origin, PIOL is predominantly a non–Hodgkin lymphoma of B-cell origin (5). Although initially presenting intraocularly, it has been reported that 60% to 85% of patients with PIOL will develop CNS lymphoma (6–8) and 15% to 25% of PCNSL patients will have ocular involvement at the time of diagnosis (9–11). In addition to the histopathlogical diagnosis, other indices that may be suitable for supporting a clinical diagnosis of PIOL include the absolute level of vitreous interleukin (IL)-10, or the vitreous IL-10 to IL-6 ratio, and the rearrangement of *IgH* genes in the tumor cells (12,13). However, the molecular pathogenesis of PIOL is still poorly understood, partially due to the lack of a suitable model. In addition, effective therapies for this disease are wanting. A recent report on a mouse intraocular lymphoma model is promising; however, it is a murine T-cell PIOL (14).

Recombinant immunotoxin therapy is an emerging and novel immunotherapeutic approach (15). Immunotoxins are recombinant proteins that combine cytotoxicity of an exotoxin, usually a microbial exotoxin, with the specificity of a monoclonal antibody to ensure target-specific killing. One immunotoxin that specifically targets B-cell lymphoma is immunotoxin RFB4 (dsFv)-PE38 (BL22; ref. 16). BL22 is a hybrid protein that contains a binding domain from a monoclonal antibody that specifically recognizes the B cell–specific surface marker CD22, which is covalently linked to a portion of P*seudomonas* exotoxin A. After specifically binding to B cells that express CD22, the exotoxin (*Pseudomonas* exotoxin) is internalized, translocated, ADP-ribosylated, and eventually causes cell death. BL22 has been used in clinical trial for chemotherapy-resistant, hairy-cell leukemia, and shows great potential (17). Immunotoxin HA22 is a mutated form (R409A) of BL22 with increased antitumor activity without an increase in animal toxicity (18).

In this study, we established a murine model resembling primary human B-cell intraocular lymphoma and used the immunotoxin HA22 to treat the intraocular lymphoma. The new murine intraocular lymphoma model using a human B-cell lymphoma cell line closely mimics human PIOL. A single intravitreous injection of HA22 in the eye with lymphoma resulted in complete regression of the tumor.

Materials and Methods

Cell culture and reagents

A human B lymphoma cell line (CA46) from American Type Culture Collection (Mannasas, VA) was cultured and maintained in culture medium [RPMI 1640 with 10% fetal bovine serum, 1× nonessential amino acids, 1× antibiotics (penicillin and streptomycin), and 2 mmol/L glutamine] at 37°C in 5% CO_2. Cell density was maintained between 4×10^5/mL and 6×10^5/mL. Recombinant immunotoxin HA22 was expressed and purified as described earlier (18). A nonspecific immunotoxin (erb-38) that does not bind human normal as well as malignant B cells as a control immunotoxin was also expressed and purified as described earlier (19,20).

Animals, intravitreous injection, and fundoscopic examination

Severe combined immune deficiency (SCID) mice and their wild types were purchased from The Jackson Laboratory (Bar Harbor, ME). All of the experimental procedures were approved by the Animal Care and User Committee of National Eye Institute of NIH, according to the USPHS Policy on Humane Care and Use of Laboratory Animals. Before intravitreous injection, cultured tumor cells were spun down and washed once with washing buffer [PBS, 0.2% bovine serum albumin (BSA)]. Cells were then resuspended in PBS (pH 7.3) at various concentrations and kept at room temperature before injection. For the intravitreous injection, animals were anesthetized for restraint with an i.p. injection of ketamine hydrochloride (35-50 mg/kg) and xylazine hydrochloride (5-10 mg/kg). By using a 33-gauge needle, both eyes were injected

with 2μL per eye per injection of PBS (pH 7.3) with or without either tumor cells for establishing intraocular lymphoma or immunotoxin for therapy. Animals were anaesthetized as described above plus topical application of 0.5% proparacaine. Pupils were then dilated with 1% tropicamide (Alcon Laboratories, Inc., TX) and the fundus was viewed and examined using a dissecting microscope with fiberoptic translumination.

Flow cytometry analysis

Phycoerythrin-conjugated monoclonal antibodies against CD22, CXCR4, and CXCR5 were all from BD Biosciences (San Jose, CA). For flow cytometry phenotyping of surface markers, cells were suspended at 1×10^6 per tube in staining/washing buffer (PBS with 0.5% BSA) and incubated with specific conjugated monoclonal antibodies at room temperature for 15 minutes. For intracellular IL-10 level measurements, CA46 cells were cultured as described above. After blocking with GolgiPlug (BD Biosciences) for 10 to 12 hours, cells were permeabilized using the Perm & Mix staining kit (Caltag, San Jose, CA) according to the instruction of the manufacturer and stained with human IL-10–specific antibody (Caltag) for 30 minutes. After washing with washing buffer, cells were fixed in 1% paraformaldehyde and acquired by a FACSCalibur flow cytometer (BD Bioscience). Data were analyzed using the FlowJo software (TreeStar, San Jose, CA)

Histology and immunohistochemical staining

Animal tissues were collected after euthanization at specified time points. They were fixed immediately in 4% glutaraldehyde, then transferred into 10% formalin for routine histology (H&E staining). Otherwise, freshly isolated tissues from euthanized animals were embedded in optimal cutting temperature compound (Miles Laboratory, Naperville, IL), snap-frozen on dry ice, and stored at –70°C for further examination.

For immunohistochemical staining, frozen tissue sections were cut through the pupil-optic nerve axis at 6 to 8 μm and placed on coated slides (Superfrost/Plus; Fisher Scientific, Fair Lawn, NJ). Frozen sections or cytologic slides of cultured cells were fixed in 4% paraformaldehyde for 7 minutes and treated with 10% animal serum at room temperature for 30 minutes to block nonspecific binding. The cells were incubated with phycoerythrin-labeled specific antibodies at desired concentrations for 1 hour at room temperature and counterstained with 4′,6-diamidino-2-phenylindole (DAPI). The specific binding of antibodies was analyzed using either a fluorescence microscope (Olympus, Melville, NY) or a laser scanning confocal microscope (model SP2; Leica, Microsystems, Exton, PA) equipped with Nomarski optics. Immunolabeled and negative control sections were imaged under identical scanning conditions.

Microdissection and quantitative real-time PCR

Tumor cells were manually microdissected from the stained frozen slides of eye or cytologic slides of cultured cells based on histologic and morphologic characteristics. Total RNAs from microdissected cells were extracted using a PicoPure RNA isolation kit (Acturus, Mountain View, CA) according to the instruction of the manufacturer. Each RNA sample was split evenly into two portions for real-time PCR to detect either IL-10 or CXCR4, and β-actin. Amplification of β-actin mRNA served as RNA loading control. A mouse universal RNA (BD Biosciences) was used as a normal control for quantitative assay of gene expression. Specific amplification for mouse glyceraldehyde-3-phosphate dehydrogenase (GAPDH) was done to rule out potential contamination of mouse cells in microdissected human B lymphoma cells from eye tissues. The Superscript II RNase H^- Reverse Transcriptase kit (Invitrogen-Life Technologies, Grand Island, NY) with random hexamers (Promega, Madison, WI) was used for cDNA synthesis. Real-time PCR was done using a Stratagene Mx3000 Real-time PCR System and Brilliant SYBR Green QPCR Master Mix (Stratagene, La Jolla, CA). The primers

for IL-10 and CXCR4 were synthesized by Superarray Corp. (Frederick, MD) and supplied as RT-PCR primer sets (Superarray Corp.). β-Actin as an internal control was amplified using primers 5′-CCCAGCACAATGAAGATCAA-3′ and 5′-ACATCTGCTGGAAGGTGGAC-3′. Reactions were done in a final volume of 50 μL with 2 μL of cDNA. The real-time PCR cycling conditions were as follows: 95°C for 10 minutes, followed by 45 cycles for 30 seconds at 95°C, 60 seconds at 55°C, and 30 seconds at 72°C followed by fluorescence measurement. Following PCR, a thermal melt profile was done for amplicon identification. To determine the value of threshold cycle (C_T), the threshold level of fluorescence was set manually in the early phase of the PCR amplification. The relative gene expression of tumor cell RNA compared with mouse universal RNA was presented as arbitrary units of the ratio of the C_T of the gene of interest over the C_T of β-actin gene.

Results

Human B lymphoma cell line CA46 expresses molecular markers for human PIOL

We first examined the phenotypic characteristics of B-cell lymphoma cell line (CA46) used in the establishment of our murine PIOL, including several molecular markers such as CXCR4, CXCR5, IL-10, and CD22. The expression of surface CD22 is essential for the application of immunotoxin (HA22) therapy. CXCR4, CXCR5, and IL-10 are thought to play an important role for the pathogenesis of PIOL (12,13). The surface expression of CD22, CXCR4, CXCR5, and the intracellular IL-10 expression were examined by flow cytometry. As shown in Fig. 1*A*, all CA46 cells express CD22 as well as CXCR4 and CXCR5. They also constitutively produce the B-cell growth factor/anti-inflammatory cytokine IL-10, which is thought to be an important pathogenic factor and is of diagnostic importance for human PIOL. The expression of the B-cell growth factor/anti-inflammatory cytokine IL-10 and the chemokine receptor CXCR4 was also confirmed by quantitative real-time PCR (Fig. 1*B*).

Intravitreous injection of CA46 cells induces intraocular lymphoma

After confirming the phenotypic characteristics of CA46 cells, we investigated the possibility of inducing intraocular lymphoma in mice by intravitreally injecting the CA46 cell line. Different numbers of CA46 cells (ranging from 6,000 cells per eye per injection up to 200,000 cells per eye per injection) were intravitreally injected into either SCID mice or their wild-type background mice (either BALB/c or C57BL/6 background). Animals were monitored either clinically or by fundoscopic examination. Animals were sacrificed at different time intervals from as early as 7 days up to 5 weeks. Enucleated eyes and other tissue samples, including brains, lungs, spleens, and livers, were examined macroscopically and microscopically. There was no intraocular tumor development in any of the wild-type mice (data not shown), whereas SCID mice showed evidence of tumor establishment starting as early as day 10. Figure 2*A*illustrates an eye at day 10 after an intravitreous injection of 20,000 lymphoma cells. There were numerous tumor cells in the vitreous cavity but there was apparent colonization and invasion of tumor cells into the retina (*arrows*), suggesting establishment of the tumor. When more tumor cells were injected and eyes were examined at a later time, the intraocular lymphoma was more fully developed. As shown in Fig. 2*B*, for animals receiving an intravitreous injection of 20,000 tumor cells per eye and examined on day 21, tumor cells invaded into the retina and caused massive retinal damage.

The severity of the mouse B-cell intraocular lymphoma depends on both the time after intravitreous injection and the number of tumor cells originally injected. Table 1 summarizes the information regarding time and cell numbers for intravitreous injections that were essential for establishing intraocular lymphoma when using CA46 cells and SCID mice as a model. These data were compiled from more than six independent animal studies. Our experience showed that with a minimum of 20,000 tumor cells injected intravitreally into SCID mice,

100% of the mice would develop clinically apparent intraocular lymphoma starting as early as on day 10. The tumor would continuously grow and invade the retina as well as the choroid.

The murine B-cell intraocular lymphoma model mimics human PIOL

The ocular histology of CA46 cells induced murine intraocular lymphoma revealed that the tumor cells could further infiltrate into retina after initial colonization and invasion. Interestingly, we observed that the tumor cells seemed to preferentially penetrate and expand in the subretinal space, or known as SRS (Fig. 2*B, b, c*). In human PIOL, this is considered one of the hallmarks of human PIOL clinically and histopathologically (13). Because 60% to 80% of human PIOL will eventually develop CNS lymphoma (6–8), we examined the involvement of CNS and other nonocular tissues (liver, lungs, kidney, bones, etc.) at different stages of tumor development in this murine B-cell lymphoma model. Only the brain tissues revealed metastasis of the tumor cells at late stage. As shown in Fig. 2*C*, numerous lymphoma cells invaded the brain 35 days after tumor injection (200,000 cells per injection). The tumor cells (*arrows*) accumulated around the brain meninges and parenchyma, and were mixed with a few inflammatory cells.

The murine model may be used to study molecular pathogenesis of human PIOL

As described earlier, the human CA46 lymphoma cells resemble human primary intraocular B lymphoma cells in that they all express CD22, CXCR4, and CXCR5 and secrete cytokine IL-10. We further investigated the molecular and histopathologic resemblance of CA46 lymphoma–induced murine intraocular lymphoma to human PIOL *in vivo*. First, we examined whether the above molecules were still expressed *in vivo* after intravitreous injection and colonization/invasion into the retina. By using a combination of microdissection and real-time PCR analysis, we were able to detect molecular markers for human PIOL directly from tumor cells that colonized on and/or infiltrated into retinal tissues. As shown in Fig. 3*A*(*top*), real-time PCR analysis showed that the tumor cells expressed IL-10 typically seen in human PIOL *in vivo*. The production of IL-10 by the tumor cells infiltrated into the retina was ˜60-fold higher than that of the background level of IL-10 production. Another representative molecular marker, chemokine receptor CXCR4, was also expressed *in vivo* (*bottom*). There was no detection of mouse GAPDH from the microdissected tumor cells (data not shown) using the real-time PCR strategy, ruling out potential contamination of mouse tissues in the microdissected human tumor cells.

To further investigate the expression profiles of the molecular markers for the murine PIOL model *in vivo,*an immunohistochem-ical study was done. As shown in Fig. 3*B*, the tumor cells expressed surface CD22, CXCR4, and CXCR5 *in vivo* (red for positive staining). More intriguingly, a comparative analysis of immunohistologic staining for chemokine receptors CXCR4 and CXCR5 showed that (*a*) the expression of CXCR5 on tumor cells *in vivo* was higher than that of CXCR4 *in vivo* (comparing Fig. 3*B*, *middle* and *bottom right*); (*b*) but the CXCR5 expression on *in vitro* cultured CA46 cells was lower than that of CXCR4 (comparing Fig. 3*B*, *middle* and *bottom left*); and (*c*) flow cytometry data on *in vitro* cultured CA46 cells (Fig. 1*A*, *middle*) also showed that the expression level of CXCR5 was lower than that of CXCR4. An isotype control antibody was used to stain tissues and showed no specific staining (data not shown). Taken together, these data suggest that there was an up-regulation of CXCR5 *in vivo* in this murine PIOL model. Overlay pictures showing both DAPI staining (blue-colored for nuclei) and the antibodies staining (red-colored for CD22, or CXCR4 or CXCR5) can be seen in Supplementary Fig. S1.

A single dose injection of HA22 resulted in complete regression of the CA46 cell–induced intraocular lymphoma coupled with minimum retinal cytotoxicity

After establishing the B-cell lymphoma murine model for human PIOL, we tested the potential application of an immunotoxin (HA22) in treating intraocular lymphoma. Because immunotoxin HA22 specifically targets the surface molecule CD22, we first examined if there is a background expression of CD22 in human and mouse ocular tissues. No CD22 expression in either human or mouse ocular tissues were observed by immunohistochemical staining (data not shown). As described above, we showed that tumor cells colonized and invaded the retina 10 days after tumor injection. To mimic a clinical scenario, we started immunotoxin (HA22) therapy on day 12 after tumor injection (20,000 per injection). Various doses of HA22 (ranging from 2 to 2,000 ng per eye per injection) were intravitreally injected on 12th day postinjection of the CA46 tumor cells. Figure 4 shows a representative experiment in which the nontreated mouse eye developed full-blown intraocular lymphoma on day 21 (Fig. 4*A*), whereas mice treated with intravitreous injection of HA22 at 200 ng/eye had complete tumor regression (Fig. 4*B*). The cells shown in the vitreous were all inflammatory cells. More strikingly, there were minimal histologic changes to the retinal tissue after the HA22 injection at the effective dose (200 ng/eye/injection) for treating B-cell lymphoma. The retina remained intact under effective therapy (200 ng/eye/injection) of HA22 (Fig. 4*B*, bottom). However, at a much higher concentration (2000 ng/eye/injection) of HA22, retinal degeneration, gliosis, and atrophy were observed. As shown in Fig. 4C, an intravitreous injection of HA22 at 2,000 ng/eye achieved complete tumor regression (compare Fig. 4*C*with *A*) but it seemed to induce retinal damage in some animals (compare Fig. 4*C*with *B*). Table 2 summarizes data from three independent dose-dependent experiments for HA22 in treating this murine intraocular lymphoma. To rule out the possibility of killing of the tumor cells due to nonspecific cytotoxicity, another immunotoxin targeting a proto-oncogen product, which is not expressed on normal or malignant B cells, erb-38 (19,20), was used to treat tumor in this model. There was no therapeutic effect of this control immunotoxin (see Supplementary Fig. S2), demonstrating a B cell–specific therapeutic effect of HA22.

Discussion

A general trend toward an increasing incidence of PCNSL has been noted over the last two decades (1,21). PIOL, as a subset of PCNSL, has drawn more attention clinically (22–24). One of the great challenges for clinicians is that PIOL patients may not present with typical clinical manifestations, making it difficult to diagnose (25–27). PIOL simulates other ocular inflammatory clinical conditions and is hence called a ‘‘masquerade syndrome.’’ Patients with PIOL are often diagnosed as being a ‘‘corticosteroid-resistant idiopathic uveitis,’’ causing a delay in final diagnosis. A lack of understanding of the pathogenesis of PIOL has been recognized recently. Currently, no cell line derived from a human PIOL sample is available nor is there any animal model for intraocular human B-cell lymphoma. A mouse intraocular T lymphoma model, mimicking human PIOL, has recently been developed (14). The main concern of that murine model is the origin of the lymphoma cells being T cells, whereas the majority (98%) of human PIOL is of B-cell origin. Thus, establishing a murine intraocular lymphoma model of human B-cell origin for studying human PIOL has clinical significance. In this study, we sought to establish a murine intraocular lymphoma model by using human B-cell lymphoma cells. We reasoned that (*a*) a murine model that develops intraocular lymphoma with human B cell would mimic human PIOL more closely than the T cell would and (*b*) this model can be used directly for testing novel therapies that may have a direct clinical effect for the treatment of human PIOL.

By intravitreally injecting human B-cell lymphoma cells into SCID mice, we established a murine intraocular lymphoma model that closely mimics human B-cell PIOL. Our results show

that this model is highly reproducible and feasible. After a single injection of 20,000 cells per eye intravitreally, all the mouse eyes develop intraocular lymphoma. Moreover, fewer cells, as low as several thousand cells (Table 1), are sufficient to induce intraocular lymphoma in this model. Although relatively little is known about the molecular pathogenesis of human PIOL, several molecules have been implicated as pathogenesis factors. IL-10 has been suggested to play key role in the pathogenesis of human PIOL (13,28). PIOL cells produce high levels of IL-10, a B-cell growth factor, and anti-inflammatory cytokine. Patients with PIOL usually have a high concentration of IL-10 in the vitreous (28). The elevated level of IL-10 or a high IL-10/IL-6 ratio in the vitreous has been accepted as one of the indices for assisting the clinical diagnosis of PIOL (12,13,28,29). In addition, CXCR4 and CXCR5, the B-cell chemokine receptors, have also been suggested as potential pathogenesis factors (12, 13). We examined the expression levels of IL-10, CXCR4, and CXCR5 on the tumor cell line (CA46) that was used for establishing this mouse model. CA46 cells were shown to express all of the above potential pathogenesis factors. The CA46 cells also express CD22 on their surface, which is the molecular target for immunotoxin HA22 (Fig. 1). We then investigated the *in vivo* expression profile of the above molecules in an established tumor in this mouse model. Using both real-time PCR and immunohis-tochemical staining, we found that IL-10, CXCR4, CXCR5, and CD22 were all expressed by the tumor cells *in vivo* (Fig. 3). More interestingly, chemokine receptor CXCR5 seemed differentially regulated when the *in vitro* and *in vivo* expression profiles were compared. Although *in vitro* cultured tumor cells express more CXCR4 on their surface than CXCR5 (Fig. 1A, *middle*, and Fig. 3B,*middle* and *bottom left*), immunohistochemical staining indicated that the tumor cells expressed more CXCR5 than CXCR4 *in vivo* (Fig. 3B, *middle* and *bottom right*). These data suggested that CXCR5 was up-regulated *in vivo* in this mouse model. Although we do not understand the mechanism and biological implications for this observation, there has also been no documentation regarding the differential expression of CXCR4 and CXCR5 *in vitro* versus *in vivo* in human PIOL. CXCR5 has been known to be involved in the regulation of trafficking of normal as well as malignant B cells (30,31). Interestingly, CXCL13, the only known ligand for CXCR5, is found on the surface of human retinal pigment epithelium cells, which is part of the constituents of the SRS, and the brain tissues from PCNSL patients (32,33). Taken together, these findings suggest that the CA46 lymphoma induced murine intraocular lymphoma model resembles human PIOL in that the tumors in both systems shared similar expression profiles of certain putative pathogenesis factors.

Histologically, the CA46 cell–induced murine intraocular lym-phoma model also resembles human PIOL. One of the histopath-ologic characteristics of human PIOL is the localization of tumor cells into the SRS around retinal pigment epithelium. In the CA46 cell–induced intraocular lymphoma model, we observed a similarly preferential invasion and expansion of tumor cells in the SRS (Figs. 2*B*and 4*A*). It may suggest a more ‘‘fitting niche’’ of that region for tumor growth, or expression of certain chemoattractants as well as adhesion molecules and/or chemokines in that region, or protection from host immune responses. Indeed, the SRS in the retina has been shown a ‘‘immunoprivileged site’’ for tumors or allogeneic transplants (34). We intend to investigate the mechanism(s) of this phenomenon and this mouse model seems very applicable.

It has been estimated that 60% to 85% of human PIOL have CNS involvement. In this CA46 cell–induced murine intraocular lymphoma model, we observed metastasis of tumors into mouse brain but no signs of metastasis was observed at other sites. It seemed that this metastasis could be mediated through local infiltration, considering the proximity of eye and the direct link via the optic nerves to the brain. In fact, we found it interesting that the B lymphoma cells preferentially migrated into the optic nerve at early colonization stage (Fig. 2A).

In addition to facilitating the investigation on the molecular pathogenesis of PIOL, another main reason for us to establish this murine model was to use it for testing novel therapeutic strategies for human PIOL. Clinically, effective therapies with more potent efficiency and less cytotoxicity for treating PIOL as well as other PCNSL are being sought. The clinical treatment of PIOL has been complicated by the blood-ocular barrier that limits access of therapeutic drugs to the tumor residing under the retina. Currently, there is still debate whether isolated PIOL should be treated locally alone or systemically in conjunction with a protocol that presumes CNS involvement. Intraocular delivery of effective drugs may be an ideal option for treating PIOL without apparent evidence for CNS involvement. Immunotoxin has been developed and used as a novel strategy for treating leukemia and lymphoma (35). A recently developed immunotoxin combining a monoclonal antibody against CD22 and a *Pseudomonas* exotoxin (BL22) has been successfully used in a phase I clinical trial for treating hairy cell leukemia, achieving satisfactory therapeutic effects (17). Because PIOL is predominantly of B-cell origin and many tumors express surface CD22, an immunotoxin strategy against CD22 would be of great interest. HA22 is a mutated form of BL22 with 5- to 10-fold higher cytotoxicity on CD22-positive cells and has been shown to be up to 50 times more effective in killing tumor cells from patients with chronic lymphocytic leukemia and hairy cell leukemia (18). Besides B cells migrating into the ocular tissue, there are no known CD22-positive molecules expressed in the eye, in both human and mouse (data not shown). Therefore, HA22 constitutes an excellent investigative candidate drug for treating human PIOL. After establishing this murine model for human intraocular lymphoma, we investigated the potential of HA22 in treating intraocular lymphoma. To our satisfaction, a single dose injection of HA intravitreally resulted in complete tumor regression. Because the intravitreous injection of HA22 was delayed until tumor cells started to colonize and infiltrate into retina tissues, the therapeutic effect of HA22 seems to be very effective and clinically applicable. In addition, HA22 caused minimal cytotoxicity to normal ocular tissues when administered at its effective dosage range, e.g., 200 ng/ eye/injection (Fig. 4B). Only at doses 10 times higher than its effective dose was there a cytotoxic effect of HA22 to retinal tissues in some of the treated animals (Fig. 4C).

In summary, we have established a murine intraocular B-cell lymphoma model that closely mimics human B-cell PIOL. The newly established murine intraocular B-cell lymphoma model may provide a valuable tool for investigating molecular mechanisms of human PIOL. In addition, by using immunotoxin HA22 as a therapeutic approach, we showed that immunotoxin HA22 is a potentially potent therapy for treating intraocular B-cell lymphoma with minimal cytotoxicity to the normal retinal tissues at therapeutic dosage. The murine model may also serve as a useful tool for evaluating new novel therapeutic drugs.

Acknowledgements

Grant support: Intramural Research Program of NIH, National Eye Institute and NCI.

References

1. Eby NL, Grufferman S, Flannelly CM, Schold SC, Vogel FS Jr, Burger PC. Increasing incidence of primary brain lymphoma in the US. Cancer 1988;62:2461–5. [PubMed: 3179963]
2. Kadan-Lottick NS, Skluzacek MC, Gurney JG. Decreasing incidence rates of primary central nervous system lymphoma. Cancer 2002;95:193–202. [PubMed: 12115333]
3. Cote TR, Manns A, Hardy CR, Yellin FJ, Hartge P. Epidemiology of brain lymphoma among people with or without acquired immunodeficiency syndrome. AIDS/Cancer Study Group. J Natl Cancer Inst 1996;88:675–9. [PubMed: 8627644]
4. Brain Tumor in the United States 1995-1999. Chicago (Illinois): Central Brain Tumor Registry of the United States, 2002-2003.

5. Coupland SE, Heimann H, Bechrakis NE. Primary intraocular lymphoma: a review of the clinical, histo-pathological and molecular biological features. Graefes Arch Clin Exp Ophthalmol 2004;242:901–13. [PubMed: 15565454]
6. Corriveau C, Easterbrook M, Payne D. Lymphoma simulating uveitis (masquerade syndrome). Can J Ophthalmol 1986;21:144–9. [PubMed: 3755372]
7. Char DH, Ljung BM, Miller T, Phillips T. Primary intraocular lymphoma (ocular reticulum cell sarcoma) diagnosis and management. Ophthalmology 1988;95:625–30. [PubMed: 3050698]
8. Akpek EK, Ahmed I, Hochberg FH, et al. Intraocularcentral nervous system lymphoma: clinical features, diagnosis, and outcomes. Ophthalmology 1999;106:1805–10. [PubMed: 10485554]
9. Peterson K, Gordon KB, Heinemann MH, DeAngelis LM. The clinical spectrum of ocular lymphoma. Cancer 1993;72:843–9. [PubMed: 8334638]
10. DeAngelis LM. Primary central nervous system lymphoma. Recent Results Cancer Res 1994;135:155–69. [PubMed: 8047690]
11. Verbraeken HE, Hanssens M, Priem H, Lafaut BA, De Laey JJ. Ocular non-Hodgkin's lymphoma: a clinical study of nine cases. Br J Ophthalmol 1997;81:31–6. [PubMed: 9135405]
12. Tuaillon N, Chan CC. Molecular analysis of primary central nervous system and primary intraocular lym-phomas. Curr Mol Med 2001;1:259–72. [PubMed: 11899075]
13. Chan CC. Molecular pathology of primary intra- ocular lymphoma. Trans Am Ophthalmol Soc 2003;101:275–92. [PubMed: 14971583]
14. Chan CC, Fischette M, Shen D, Mahesh SP, Nussenblatt RB, Hochman J. Murine model of primary intraocular lymphoma. Invest Ophthalmol Vis Sci 2005;46:415–9. [PubMed: 15671263]
15. Pastan I, Beers R, Bera TK. Recombinant immuno-toxins in the treatment of cancer. Methods Mol Biol 2004;248:503–18. [PubMed: 14970517]
16. Kreitman RJ, Margulies I, Stetler-Stevenson M, Wang QC, FitzGerald DJ, Pastan I. Cytotoxic activity of disulfide-stabilized recombinant immunotoxin RFB4(dsFv)-PE38 (BL22) toward fresh malignant cells from patients with B-cell leukemias. Clin Cancer Res 2000;6:1476–87. [PubMed: 10778980]
17. Kreitman RJ, Wilson WH, Bergeron K, et al. Efficacy of the anti-CD22 recombinant immunotoxin BL22 in chemotherapy-resistant hairy-cell leukemia. N Engl J Med 2001;345:241–7. [PubMed: 11474661]
18. Bang S, Nagata S, Onda M, Kreitman RJ, Pastan I. HA22 (R490A) is a recombinant immunotoxin with increased antitumor activity without an increase in animal toxicity. Clin Cancer Res 2005;11:1545–50. [PubMed: 15746059]
19. Reiter Y, Brinkmann U, Jung SH, et al. Improved binding and antitumor activity of a recombinant antierbB2 immunotoxin by disulfide stabilization of the Fv fragment. J Biol Chem 1994;269:18327–31. [PubMed: 7913461]
20. Pai-Scherf LH, Villa J, Pearson D, et al. Hepatotoxicity in cancer patients receiving erb-38, a recombinant immunotoxin that targets the erbB2 receptor. Clin Cancer Res 1999;5:2311–5. [PubMed: 10499598]
21. Corn BW, Marcus SM, Topham A, Hauck W, Curran WJ Jr. Will primary central nervous system lymphoma be the most frequent brain tumor diagnosed in the year 2000? Cancer 1997;79:2409–13. [PubMed: 9191531]
22. Chan CC, Buggage RR, Nussenblatt RB. Intraocular lymphoma. Curr Opin Ophthalmol 2002;13:411–8. [PubMed: 12441846]
23. Davis JL. Diagnosis of intraocular lymphoma. Ocul Immunol Inflamm 2004;12:7–16. [PubMed: 15209459]
24. Levy-Clarke GA, Chan CC, Nussenblatt RB. Diagnosis and management of primary intraocular lymphoma. Hematol Oncol Clin North Am 2005;19:739–49. [PubMed: 16083834]
25. Buggage RR, Chan CC, Nussenblatt RB. Ocular manifestations of central nervous system lymphoma. Curr Opin Oncol 2001;13:137–42. [PubMed: 11307054]
26. Fahim DK, Bucher R, Johnson MW. The elusive nature of primary intraocular lymphoma. J Neuroophthalmol 2005;25:33–6. [PubMed: 15756131]
27. Kim SK, Chan CC, Wallace DJ. Management of primary intraocular lymphoma. Curr Oncol Rep 2005;7:74–9. [PubMed: 15610690]

28. Whitcup SM, Stark-Vancs V, Wittes RE, et al. Association of interleukin 10 in the vitreous and cerebrospinal fluid and primary central nervous system lymphoma. Arch Ophthalmol 1997;115:1157–60. [PubMed: 9298057]

29. Buggage RR, Whitcup SM, Nussenblatt RB, Chan CC. Using interleukin 10 to interleukin 6 ratio to distinguish primary intraocular lymphoma and uveitis. Invest Ophthalmol Vis Sci 1999;40:2462–3. [PubMed: 10476821]

30. Muller G, Hopken UE, Stein H, Lipp M. Systemic immunoregulatory and pathogenic functions of homeostatic chemokine receptors. J Leukoc Biol 2002;72:1–8. [PubMed: 12101256]

31. Lopez-Giral S, Quintana NE, Cabrerizo M, et al. Chemokine receptors that mediate B cell homing to secondary lymphoid tissues are highly expressed in B cell chronic lymphocytic leukemia and non-Hodgkin lymphomas with widespread nodular dissemination. J Leukoc Biol 2004;76:462–71. [PubMed: 15155773]

32. Chan CC, Shen D, Hackett JJ, Buggage RR, Tuaillon N. Expression of chemokine receptors, CXCR4 and CXCR5, and chemokines, BLC and SDF-1, in the eyes of patients with primary intraocular lymphoma. Ophthalmology 2003;110:421–6. [PubMed: 12578791]

33. Smith JR, Braziel RM, Paoletti S, Lipp M, Uguccioni M, Rosenbaum JT. Expression of B-cell-attracting chemokine 1 (CXCL13) by malignant lymphocytes and vascular endothelium in primary central nervous system lymphoma. Blood 2003;101:815–21. [PubMed: 12393412]

34. Streilein JW, Ma N, Hartmut H, Fong TF, Zamiri P. Immunobiology and privilege of neuronal retina and pigment epithelium transplants. Vision Res 2002;42:487–95. [PubMed: 11853765]

35. Pastan I, FitzGerald D. Recombinant toxins for cancer treatment. Science 1991;254:1173–7. [PubMed: 1683495]

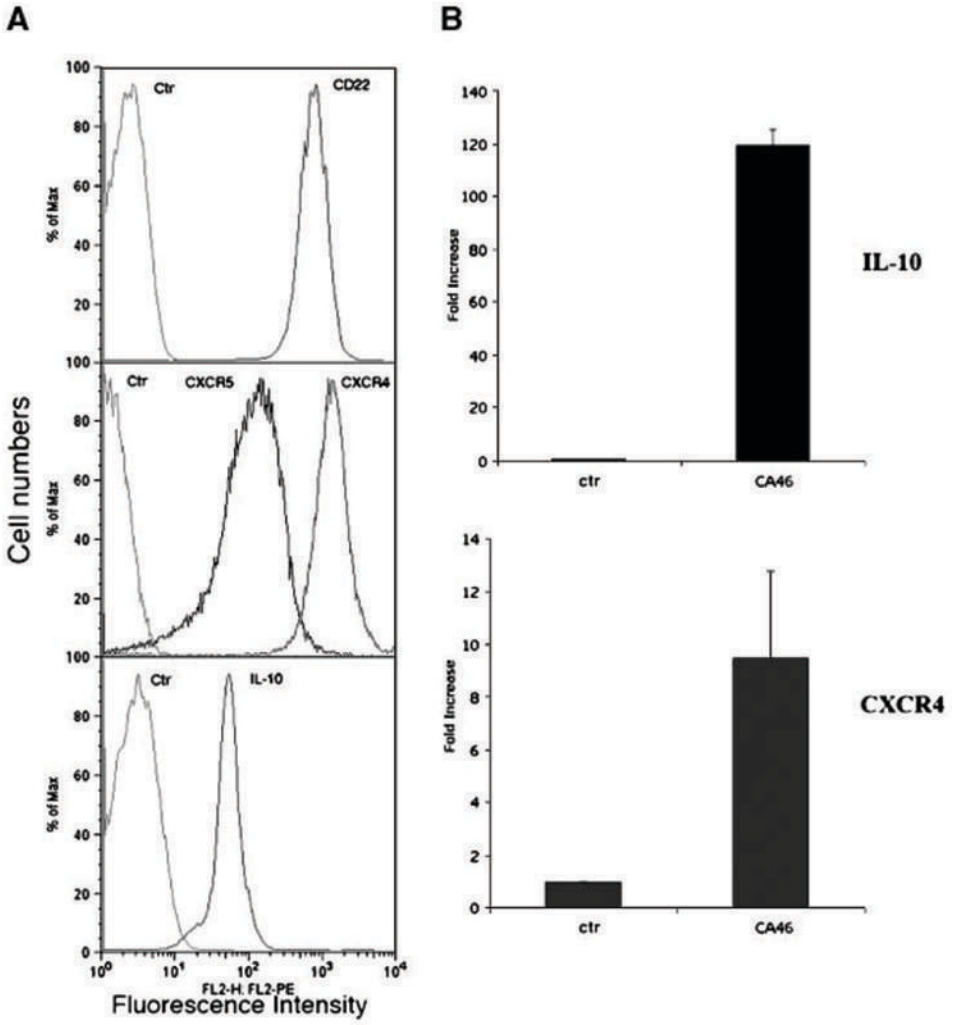

Figure 1.

Human B-cell lymphoma cell line CA46 expresses CD22, CXCR4, CXCR5, and IL-10. CA46 cells were cultured and maintained *in vitro* as described in Materials and Methods. *A*, cultured cells were analyzed for surface expression of CD22 (*top*), CXCR4 and CXCR5 (*middle*), or intracellular staining for IL-10 (*bottom*) by flow cytometry. *X* axis, relative fluorescence intensity (expression level). *Y*-axis, relative cell numbers. *B*, total RNA was isolated from cultured cells and mRNA levels of IL-10 and CXCR4 were measured by a quantitative real-time PCR as described. The levels of mRNA were expressed as the fold increase of that measured in RNA isolated from CA46 cells over that of the control RNA (mouse universal RNA). The calculation of the fold increase was detailed in Materials and Methods.

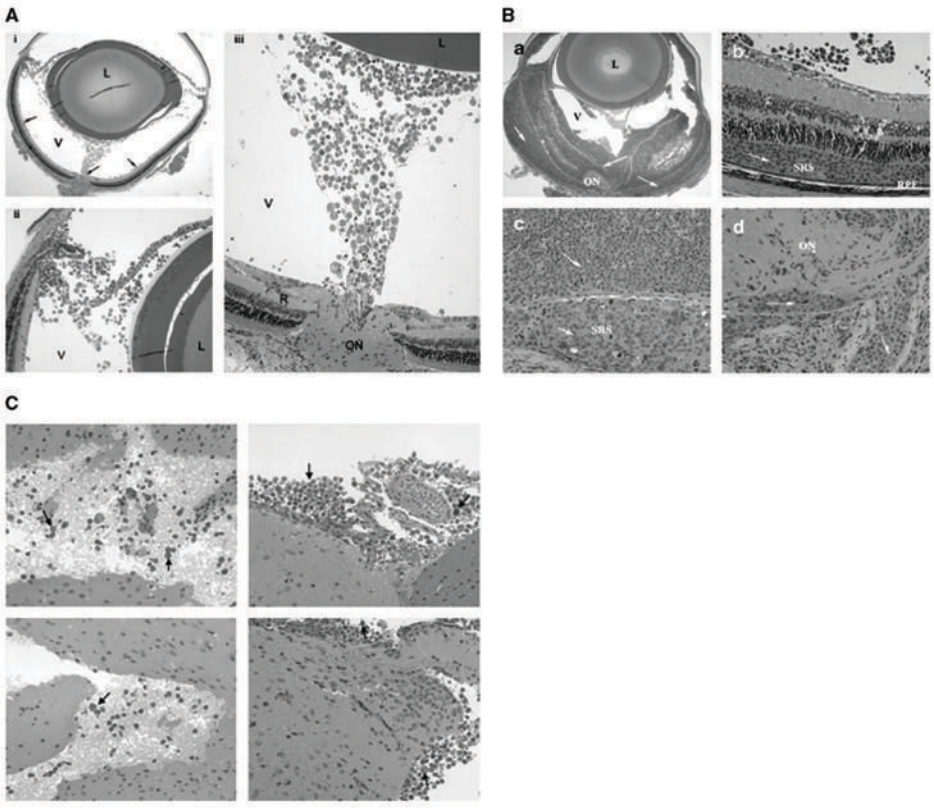

Figure 2.

Histopathology of murine intraocular B lymphoma. Cultured CA46 cells were intravitreally injected into SCID mice at different doses. Eye tissues were collected at various time points postinjection, sectioned, and stained for H&E. *A*, typical early phase (day 10 postintravitreous injection of 20,000 CA46 cells per eye) histopathology of the mouse intraocular lymphoma. Note the tumor cells in the vitreous beginning to colonize, invading into the retina and optic nerve head (*i, arrows*). Most of the retinal tissue remains intact. *ii* and *iii*, the same picture at higher magnifications. *L*, lens; *V*, vitreous; *R*, retina; *ON*, optic nerve. *B*, late-phase (day 21 postintravitreous injection of 20,000 CA46 cells per eye) histopathology of the mouse intraocular lymphoma. *a*, tumor cells infiltrating the retinal layers causing massive tissue damage. *b* and *c*, magnified views of the retina showing the preferential expansion of tumor cells (*arrows*) into the subretinal space (*SRS*). Note that the tumor cells invading the retina lie between the retinal photoreceptors and retinal pigment epithelium (*RPE; b*). *d*, tumor colonization and invasion in the optic nerve head. *Arrows*, tumor cells. *C*, metastasis of tumor cells into CNS. CA46 cells (200,000 per eye per injection) were inoculated into the eyes of SCID mice. Brain tissues were collected on day 35 and processed for histopathology. The tumor cells (*arrows*) invaded into brain tissues, accumulated around the meningeal and parenchymal brain, and were mixed with a few inflammatory cells.

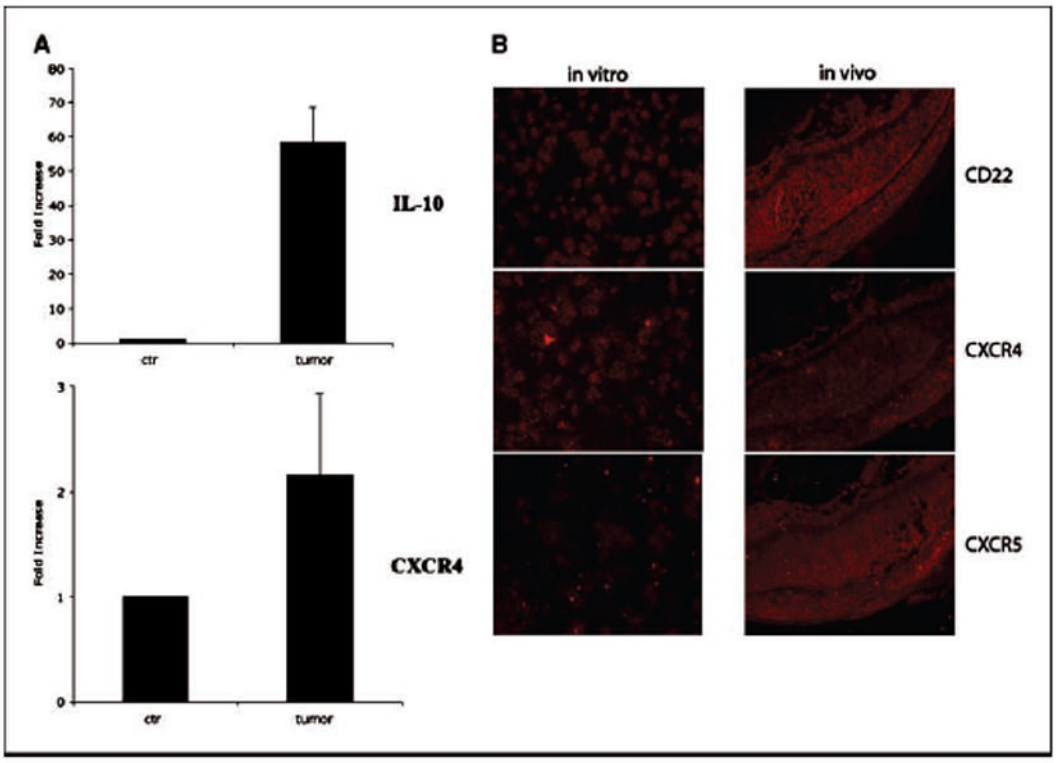

Figure 3.

Molecular mimicry of mouse intraocular B-cell lymphoma model to human PIOL. CA46 cells were intravitreally injected into SCID mice (20,000 per eye per injection), animals were sacrificed on day 21 postinjection, and eyes were collected and snap-frozen on dry ice. The frozen eye tissues were sectioned and stained for tumor cells. The tumor cells were microdissected out from the eye section, total RNA was isolated, and real-time PCR was done as described in Materials and Methods. *A*, *in vivo* expression of both IL-10 (*top*) and CXCR4 (*bottom*) in the tumor cells. *B*, immunohistochemistry shows *in vivo* expression of CD22, CXCR4, and CXCR5 on the tumor cells. *Left*, expression levels of CD22, CXCR4, and CXCR5 in the *in vitro* cultured tumor cells. *Right*, *in vivo* expression levels in the mouse tissue after injection on day 21 (*red*, positive staining). All molecular markers are expressed *in vivo* and the expression of CXCR5 seems to be up-regulated in vivo (see Results and Discussion for details). Overlay pictures showing both DAPI staining (*blue*, nuclei) and the antibody staining (*red*, CD22, or CXCR4 or CXCR5) can be seen in Supplementary Fig. S1.

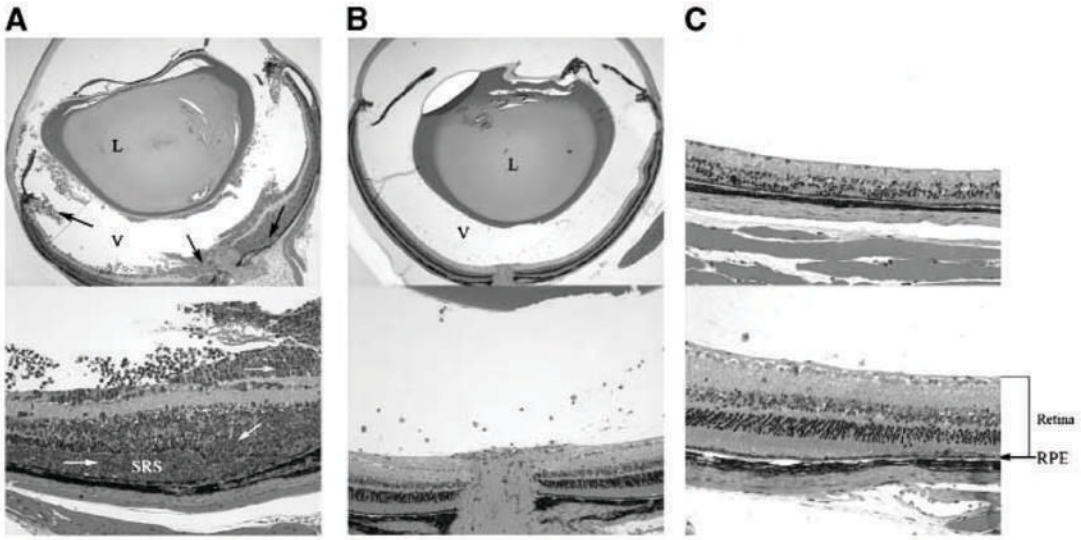

Figure 4.

Therapeutic effect of intravitreous injection of an immunotoxin targeting on surface CD22. Murine intraocular B-cell lymphoma was induced (20,000 tumor cells per injection per eye) and treated with either control vehicle [PBS (pH 7.3)] or immunotoxin HA22 at various dosages on day 12 posttumor injection as described in the text; eye tissues were collected on day 21 and processed for histopathology.*A*, histopathology of ocular tissue in mice treated with control vehicle [PBS (pH 7.3)]. There is widespread colonization and invasion of tumor cells (*arrows*) and massive retina damage.*B*, mice treated with HA22 at 200 ng/eye/injection. There was no tumor colonization and invasion into the retina tissue but only inflammatory cells, suggesting a clearing process of tumors by the immunotoxin. Note also that there is no visible retinal damage by therapy (*bottom*).*C*, two representative animals treated with higher dose of HA22 (2,000 ng/mL). Again, no tumor was observed after immunotoxin treatment.*Top*, representative of some of the mice that had substantial retinal damage after high-dose HA22 treatment;*bottom*, some of the mice that showed relative milder retinal damage. There was no therapeutic effect when a control immunotoxin, erb-38, was used (see Supplementary Fig. S2).

Table 1

Time course of tumor development

Time (d)*	Colonization	Invasion	Tissue damage	Metastasis
<10	–	–	–	–
10	+	+/–	–	–
15	+	+	+	–
>21	+	+	+	+
Dose dependence of intravitreous inoculation for tumor development				
Cell number†	Colonization	Invasion	Tissue damage	Metastasis
<6,000	–	–	–	–
6,000-20,000	+	+/–	+/–	–
>20,000	+	+	+	+

NOTE: Data are collection of six independent experiments.

*Time after tumor injection.

†Total cell numbers per eye per intravitreous injection.

Table 2

Dose response of HA22 in the treatment of intraocular lymphoma

HA22 (ng/eye)	Animals	Tumor development	Ocular tissue damage
0	1	+	–
	2	+	–
	3	+	–
	4	+	–
	5	+	–
2	1	+	–
	2	+	–
	3	+	–
	4	+	–
	5	+	–
20	1	+	–
	2	+	–
	3	+	–
	4	+	–
	5	+	–
200	1	–	–
	2	–	–
	3	–	–
	4	–	–
	5	–	–
2,000	1	–	+/ –
	2	–	+
	3	–	+
	4	–	+/ –
	5	–	+

NOTE: Data are representative of three independent experiments.